Semiconductor Physics, Quantum Electronics & Optoelectronics, 2024. V. 27, No 2. P. 216-223.

Optoelectronics and optoelectronic devices

Properties of focused combined modes of terahertz laser

A.V. Degtyarev, M.M. Dubinin*, O.V. Gurin, V.O. Maslov, K.I. Muntean, V.N. Ryabykh, V.S. Senyuta, O.O. Svystunov

V. Karazin Kharkiv National University, 4 Svobody Sq., 61022 Kharkiv, Ukraine
**Corresponding author e-mail: mykola.dubinin@karazin.ua*

Abstract. Physical features of spatial-energy characteristics of linearly polarized THz laser beams at sharp and moderate focusing in free space are analyzed both theoretically and experimentally. The Rayleigh–Sommerfeld vector theory is used to model propagation of laser beams excited by quasi-optical waveguide resonator modes in free space. Well-known methods of measuring spatial-energy characteristics of laser beams in the THz range are used in the experimental study. It is shown that the intensity of the total electric field of both combined $TE_{0n} + EH_{2n}$ and $EH_{-1n} + EH_{3n}$ modes (n = 1, 2, 3) in the focal region is defined by all three components and has a dip on the axis for both focusing types. The central maxima of the field of these modes become significantly shifted from the geometric foci of the lenses used as the order n of these modes increases. The $EH_{-11} + EH_{31}$ mode has the smallest diameter (2.94λ) of the focal spot in the maximum intensity region at sharp focusing. The $TE_{01} + EH_{21}$ mode has the smallest diameter (13.65λ) of the focal spot at moderate focusing.

Keywords: terahertz laser, dielectric resonator, combined modes, polarization, focusing.

https://doi.org/10.15407/spqeo27.02.216
PACS 42.55.-f, 42.60.-v

Manuscript received 19.01.24; revised version received 26.03.24; accepted for publication 19.06.24; published online 21.06.24.

1. Introduction

In the last decade, there has been a significant growth in research related to the terahertz (THz) range of electromagnetic radiation [1, 2]. To date, many terahertz laser sources ranging from milliwatt femtosecond laser-based generators to free electron lasers with average power of hundreds of watts [3] have been developed. Due to the high oscillation frequency, THz fields are promising for applications such as high-speed radio communication [4] including interplanetary one [5], radars [6], introscopy [7], high-resolution microscopy [8], *etc*. At the same time, due to the low photon energy, THz radiation is non-ionizing, which is a great advantage for medical applications [9], biological engineering [10], and spectroscopy of organic compounds [11].

However, application of the THz technologies has not yet reached its potential due to the lack of compact and powerful sources of THz radiation in a wide spectral range. Therefore, both development and investigation of lasers emitting in the THz range are still hot topics [12, 13]. Research on selecting and focusing THz laser beams is also topical today. Most of the works in this area deal with the optical range [14–17]. Recently, inhomogeneously polarized laser beams have attracted an increased attention [18–20]. Use of phase-sensitive electro-optical detection enables selective determination of different spatial components of the field. Longitudinal components of focused THz beams having both linear and radial polarization were obtained [21]. A longitudinally polarized wave obtained by focusing a THz beam was also studied [22]. Focusing of total electric fields by planar lenses based on super-oscillation has been proposed in [23]. The physical laws of formation and focusing of lower transverse modes of a waveguide THz laser were established [24]. It is also known that waveguide gas lasers efficiently generate combined modes that have a more complex spatial field distribution [25]. However, the properties of the combined modes of waveguide resonators have not been studied. Such beams can be useful in solving the problems of sharp focusing and super-resolution.

This work is devoted to the study of spatial-energy characteristics of combined modes generated by a THz laser whose resonator contains a hollow dielectric circular waveguide. The main attention is paid to the study of the spatial structure of radiation beams formed by combined $TE_{0n} + EH_{2n}$ and $EH_{-1n} + EH_{3n}$ (n = 1, 2, 3) modes. Both propagation of the formed beams in free space and their moderate and sharp focusing by long- and short-focal distance lenses are considered.

2. Theoretical relations

Throughout this study, the Rayleigh–Sommerfeld vector theory [26] is used to describe propagation of the laser modes in free space. These modes are the ones of a circular hollow dielectric waveguide [27]. The geometry of the laser beam focusing problem is shown in Fig. 1. We assume that the z-axis of the coordinate system is aligned with the axis of the laser beam. The coordinates origin is set in the plane of the laser output mirror, which is aligned with the end of a circular dielectric waveguide with an aperture of the diameter $2a_1$. The focusing lens of the aperture $2a_2$ is placed at some distance z_1 from the laser mirror.

The radial and azimuthal components of the $TE_{0n} + EH_{2n}$ and $EH_{-1n} + EH_{3n}$ (n = 1, 2, 3) modes in the plane of the output laser mirror (z = 0) can be described by the following expressions [25]:

$$\begin{cases} E_r(r,\phi) = A_{0n} J_1\left(\chi_{0n}\dfrac{r}{a_1}\right)\sin 2\phi, \\ E_\phi(r,\phi) = A_{0n} J_1\left(\chi_{0n}\dfrac{r}{a_1}\right)(1+\cos 2\phi), \end{cases} \tag{1}$$

for the $TE_{0n} + EH_{2n}$ modes and

$$\begin{cases} E_r(r,\phi) = B_{3n} J_2\left(\chi_{3n}\dfrac{r}{a_1}\right)[-\sin\phi + \sin 3\phi], \\ E_\phi(r,\phi) = B_{3n} J_2\left(\chi_{3n}\dfrac{r}{a_1}\right)[\cos\phi + \cos 3\phi], \end{cases} \tag{2}$$

for the $EH_{-1n} + EH_{3n}$ modes.

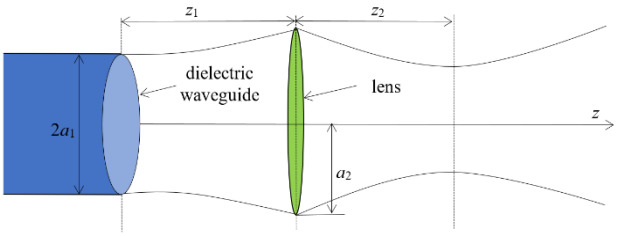

Fig. 1. Theoretical scheme of the calculation model of laser beam focusing.

Here, $A_{0n} = \dfrac{1}{\sqrt{2\pi}\,J_2(\chi_{0n})}$ and $B_{3n} = \dfrac{1}{a\sqrt{2\pi}\,J_3(\chi_{3n})}$ are the normalizing factors, J_n is the Bessel function of the first kind, and χ_{nm} is the m-th root of the equation $J_{n-1}(\chi_{nm}) = 0$, respectively.

Based on Eqs. (1) and (2), we determine the components of the modes under study on the lens aperture using the nonparaxial Rayleigh–Sommerfeld vector theory [26]. For simplicity, we assume that the focusing lens is a flat phase corrector [28]. Then, based on the obtained expressions for the field components in the plane of the phase corrector and considering its influence on the field phase, we calculate the components of the electric field of interest in an arbitrary point of the space behind the corrector in a similar way.

It is known [29] that longitudinal z-component of the field absent in an incident beam appears in the focal region of the lens. Hence, the radial and azimuthal field components of the linearly polarized combined $TE_{0n} + EH_{2n}$ modes in the focal region of the lens are accompanied by appearance of a z-component and are given by:

$$\begin{cases} E_r(\rho_2,\theta_2,z_2) = \dfrac{-ik^2 z_1 z_2}{\xi_2^2}\exp(ik\xi_2)\sin(\theta_2)A_{2n}\displaystyle\int_0^{a_2}\frac{\exp(ik\xi_1)}{\xi_1^2}\int_0^{a_1} J_1\left(\chi_{0n}\frac{r}{a_1}\right)J_1(\gamma_1 r)\exp\left(\frac{ikr^2}{2\xi_1}\right)rdr\, J_1(\gamma_2\rho_1)\times \\ \qquad \times\exp\left(\dfrac{ik\rho_1^2}{2\xi_2}\right)Ph(\rho_1)\rho_1 d\rho_1, \\ E_\phi(\rho_2,\theta_2,z_2) = \dfrac{-ik^2 z_1 z_2}{\xi_2^2}\exp(ik\xi_2)\cos(\theta_2+1)A_{2n}\displaystyle\int_0^{a_2}\frac{\exp(ik\xi_1)}{\xi_1^2}\int_0^{a_1} J_1\left(\chi_{0n}\frac{r}{a_1}\right)J_1(\gamma_1 r)\exp\left(\frac{ikr^2}{2\xi_1}\right)rdr\, J_1(\gamma_2\rho_1)\times \\ \qquad \times\exp\left(\dfrac{ik\rho_1^2}{2\xi_2}\right)Ph(\rho_1)\rho_1 d\rho_1, \\ E_z(\rho_2,\theta_2,z_2) = \dfrac{ik^2 z_1}{\xi_2^2}\exp(ik\xi_2)\sin(\theta_2)A_{2n}\displaystyle\int_0^{a_2}\frac{\exp(ik\xi_1)}{\xi_1^2}\int_0^{a_1} J_1\left(\chi_{0n}\frac{r}{a_1}\right)J_1(\gamma_1 r)\exp\left(\frac{ikr^2}{2\xi_1}\right)rdr\times \\ \qquad \times[\rho_1 J_2(\gamma_2\rho_1) - i\rho_2 J_1(\gamma_2\rho_1)]\exp\left(\dfrac{ik\rho_1^2}{2\xi_2}\right)Ph(\rho_1)\rho_1 d\rho_1, \end{cases} \tag{3}$$

The set of the field components of the linearly polarized combined $EH_{1n} + EH_{3n}$ modes in the lens focal region also includes the z-component:

$$
\begin{cases}
E_r(\rho_2,\theta_2,z_2)=\dfrac{k^2 z_1 z_2}{\xi_2^2}\exp(ik\xi_2)B_{3n}\displaystyle\int_0^{a_2}\frac{2\exp(ik\xi_1)}{\xi_1^2}\int_0^{a_1}J_2\left(\chi_{3n}\frac{r}{a_1}\right)J_1(\gamma_2 r)\exp\left(\frac{ikr^2}{2\xi_1}\right)rdr\times \\
\quad\times\left[J_3(\gamma_2\rho_1)\sin(3\theta_2)-J_1(\gamma_2\rho_1)\sin(\theta_2)\right]\exp\left(\frac{ik\rho_1^2}{2\xi_2}\right)Ph(\rho_1)\rho_1 d\rho_1, \\
E_\phi(\rho_2,\theta_2,z_2)=\dfrac{k^2 z_1 z_2}{\xi_2^2}\exp(ik\xi_2)B_{3n}\displaystyle\int_0^{a_2}\frac{2\exp(ik\xi_1)}{\xi_1^2}\int_0^{a_1}J_2\left(\chi_{3n}\frac{r}{a_1}\right)J_1(\gamma_2 r)\exp\left(\frac{ikr^2}{2\xi_1}\right)rdr\times \\
\quad\times\left[J_3(\gamma_2\rho_1)\cos(3\theta_2)+J_1(\gamma_2 r)\cos(\theta_2)\right]\exp\left(\frac{ik\rho_1^2}{2\xi_2}\right)Ph(\rho_1)\rho_1 d\rho_1, \\
E_z(\rho_2,\theta_2,z_2)=\dfrac{-k^2 z_1}{\xi_2^2}\exp(ik\xi_2)B_{3n}\displaystyle\int_0^{a_2}\frac{\exp(ik\xi_1)}{\xi_1^2}\int_0^{a_1}J_1\left(\chi_{3n}\frac{r}{a_1}\right)J_1(\gamma_2 r)\exp\left(\frac{ikr^2}{2\xi_1}\right)rdr\times \\
\quad\times\left[\,J_3(\gamma_2\rho_1)\sin(3\theta_2)-J_1(\gamma_2\rho_1)\sin(\theta_2)\right]\rho_2\exp\left(\frac{ik\rho_1^2}{2\xi_2}\right)Ph(\rho_1)\rho_1 d\rho_1.
\end{cases}
\tag{4}
$$

Here, $k=2\pi/\lambda$ is the wave number, λ is the laser wavelength, z_1 is the distance between the output mirror of the laser resonator and the lens, z_2 is the distance between the phase corrector plane and the observation plane, ρ_1, θ_1, z_1 are the cylindrical coordinates in the phase corrector plane, $\xi_1=\sqrt{z_1^2+\rho_1^2}$, $\gamma_1=k\rho_1/\xi_1$, and ρ_2, θ_2, z_2 are the cylindrical coordinates in the observation plane behind the phase corrector, $Ph(\rho_1)=\exp\left(-i\pi\rho_1^2/\lambda F\right)$ is the phase correction function of the lens, and F is the focal length of the lens, respectively.

3. Calculations results and analysis

The total electric field intensities of the investigated combined modes $I(\rho_2,\theta_2,z_2)=|E_r|^2+|E_\phi|^2+|E_z|^2$ at sharp and moderate focusing [30] were calculated by Eqs (3) and (4). The radiation wavelength λ = 0.4326 mm (THz laser generation line at optical pumping on formic acid molecule HCOOH) was chosen. The following parameter values were accepted: the waveguide length L = 1848 mm, the lens radius a_2 = 25 mm, and the waveguide radius a_1 = 17.5 mm. The focal length of the lens F = 160 mm was set according to the moderate focusing conditions (numerical aperture of the lens [31] was NA = 0.16). The sharp focusing value was chosen to be F = 36.36 mm (NA = 0.68).

The transverse distribution of the total electric field intensity for the $TE_{03}+EH_{23}$ and $EH_{-1}+EH_{33}$ modes in free space in the plane z = 300 mm behind the laser exit mirror is shown in Fig. 2. These combined modes have the largest divergence among all the studied ones.

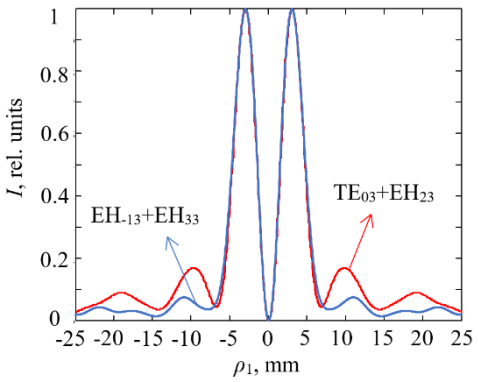

Fig. 2. Calculated transverse distributions of the total field intensity of the $TE_{03}+EH_{23}$ and $EH_{-13}+EH_{33}$ modes in free space at a distance of 300 mm from the laser output mirror.

Table. Focal spot diameters in the positions of the field intensity maximum and values of these positions for combined modes.

Types of modes	NA = 0.68		NA = 0.16	
	z_{Imax}/λ	d_σ/λ	z_{Imax}/λ	d_σ/λ
$TE_{01}+EH_{21}$	1.48	4.15	11.56	13.65
$TE_{02}+EH_{22}$	3.79	8.36	36.98	26.74
$TE_{03}+EH_{23}$	4.95	14.10	64.72	43.30
$EH_{-11}+EH_{31}$	2.06	2.94	36.98	14.58
$EH_{-12}+EH_{32}$	6.10	4.27	115.58	24.21
$EH_{-13}+EH_{33}$	8.41	5.24	196.49	33.81

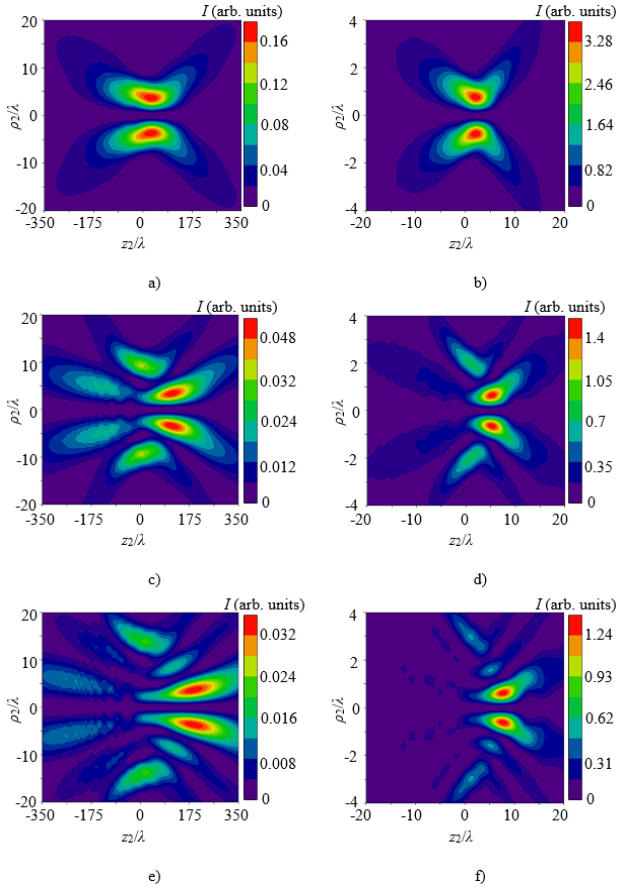

Fig. 3. Calculated distributions of the total field intensity of the $TE_{01} + EH_{21}$ (a, b), $TE_{02} + EH_{22}$ (c, d) and $TE_{03} + EH_{23}$ (e, f) modes at moderate (a, c, e) and sharp (b, d, f) focusing in the focal region of the lens.

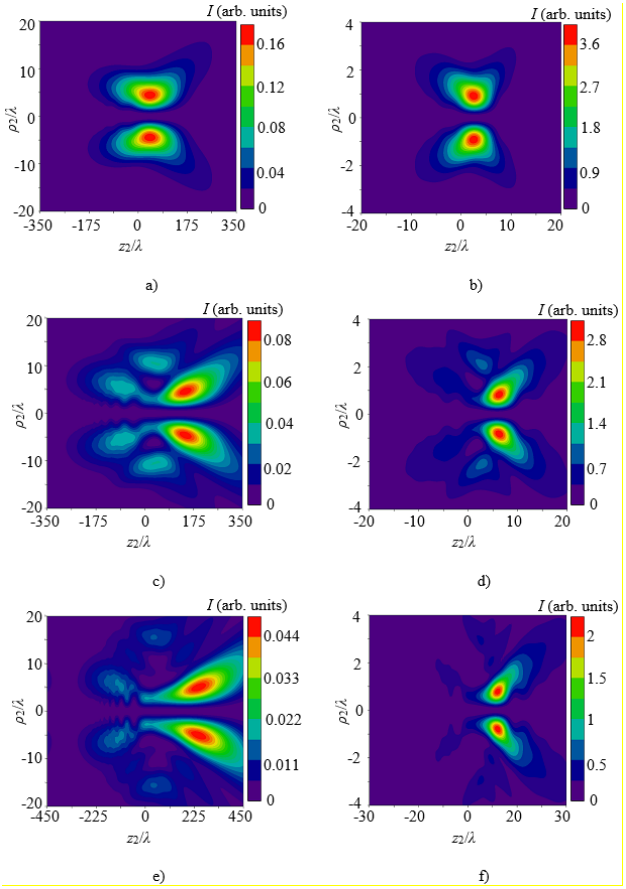

Fig. 4. Calculated distributions of the total field intensity of the $EH_{-11} + EH_{31}$ (a, b), $EH_{-12} + EH_{32}$ (c, d) and $EH_{-13} + EH_{33}$ (e, f) modes at moderate (a, c, e) and sharp (b, d, f) focusing in the focal region of the lens.

Nevertheless, as follows from Fig. 2, the lens with an aperture of 50 mm covers almost completely the radiation of the studied modes at the indicated distance.

The calculations show that the focused modes under study form several-ring structures of different intensities in the focal region of the lens. In the meridional cross section of the laser beam, these structures look like a set of individual symmetrical lobes corresponding to the areas of increased radiation intensity. A typical meridional cross section of the field intensity distribution of the combined linear polarized $TE_{0n} + EH_{2n}$ (n = 1, 2, 3) modes at sharp and moderate focusing is shown in Fig. 3.

The calculation results for the effective diameters of radiation beams in the plane of location of the intensity maxima of the $EH_{-1n} + EH_{3n}$ and $TE_{0n} + EH_{2n}$ modes as well as the displacement z_{Imax} of the intensity maxima of these modes (relative to the focal plane of the lens) are presented in Table.

The calculated intensity distributions of the total fields of combined linearly polarized $EH_{-1n} + EH_{3n}$ modes (n = 1, 2, 3) at sharp and moderate focusing are shown in Fig. 4. One can see from the figure that the total field intensity distribution of these modes and the combined $TE_{0n} + EH_{2n}$ modes have a dip on the optical axis at both focusing types. Moreover, the central lobes of the mode are also shifted both from the focal plane and from the optical axis of the radiation beam like in the previous case of the $TE_{0n} + EH_{2n}$ modes.

4. Comparison of experimental and numerical results

The numerical results were experimentally verified using a setup described in [32]. The setup contained a waveguide gas laser based on formic acid HCOOH vapor, which had strong emission lines in the THz range. The THz laser was optically pumped by a cw CO_2 laser described in [33]. The optical resonator of the THz laser contained an input phase shifter and an output flat translucent mirror with a circular hollow dielectric waveguide placed between the mirrors [32]. The current configuration of the resonator favored preferential formation and selection of combined laser modes. The spectrum of the generated laser modes is shown in Fig. 5. The radiation was registered by a pyroelectric photo-detector equipped with a pinhole diaphragm 0.2 mm in diameter.

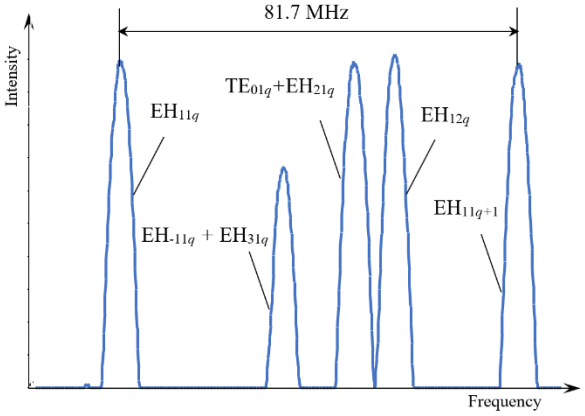

Fig. 5. Mode spectrum of the HCOOH laser.

The generation power of the EH_{11q} and $TE_{01q} + EH_{21q}$ modes of the THz laser was 3.6 mW, while the generation power of the $EH_{-11q} + EH_{31q}$ and EH_{12q} modes was 2.9 mW. The laser was set to generate the more powerful linearly polarized $TE_{01q} + EH_{21q}$ mode to study sharp and moderate focusing of the combined modes. The focal lengths of the short-focus and the long-focus lens were 36.36 mm and 160 mm, respectively.

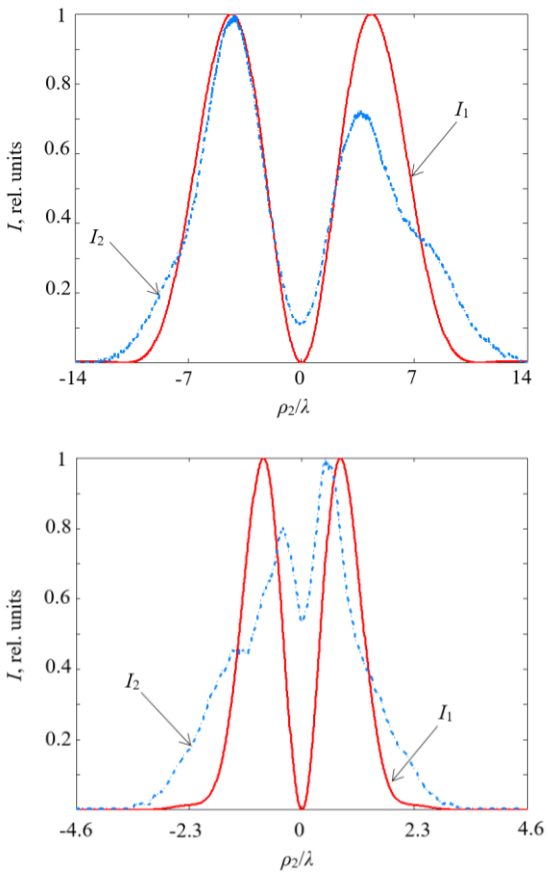

Fig. 6. Calculated (I_1) and experimental (I_2) transverse distributions of the total field intensity of the $TE_{01q} + EH_{21q}$ mode under moderate (a) and sharp (b) focusing.

The lens used in the experimental setup was mounted 300 mm from the output mirror of the THz laser providing full coverage of the laser beam. Transverse distribution of the radiation of the studied mode was measured for both sharp and moderate focusing type.

It is found both theoretically and experimentally that the plane of the $TE_{01q} + EH_{21q}$ mode field intensity peak at moderate focusing is shifted from the lens focal plane by a distance $z_{Imax} = 11.56\lambda$ in the z direction. A similar shift of the peak intensity plane for the same mode at sharp focusing is only $z_{Imax} = 1.48\lambda$. The transverse intensity distributions in the plane of the field intensity peak for the focused combined $TE_{01q} + EH_{21q}$ mode at moderate and sharp focusing are shown in Fig. 6. The panels of Fig. 6 show that the transverse intensity distribution of the $TE_{01q} + EH_{21q}$ mode maintains its circular shape in the region of the minimum size of the focused beams regardless of whether the focusing is moderate or sharp. The calculated and experimental distributions of the intensity of the focused $TE_{01q} + EH_{21q}$ mode slightly diverge. This discrepancy in the intensity distributions may be explained by the influence of lens aberrations, which were not considered in the calculations, as well as by the insufficient resolution of the photodetector.

The experiment showed that the diameter of the focused $TE_{01q} + EH_{21q}$ mode (FWHM) at moderate focusing (NA = 0.16) was 12.9λ (notice that FWHM = 13.6λ in the calculations), while this diameter at sharp focusing (NA = 0.68) was 2.2λ (notice that FWHM = 2.55λ in the calculations).

5. Conclusions

Physical features of spatial and energy characteristics of linearly polarized THz laser beams are analyzed theoretically and experimentally. The beams are excited by combined modes of a waveguide dielectric hollow laser resonator at both sharp and moderate focusing in free space.

It is shown that the intensity of the total electric field of the combined $TE_{0n} + EH_{2n}$ and $EH_{-1n} + EH_{3n}$ modes is determined by all three spatial components. The central field maxima of these modes become considerably displaced from the geometric foci of the studied lenses when the order n increases. The $EH_{-11} + EH_{31}$ mode has the smallest focal spot diameter in the region of maximum intensity at sharp focusing, while the $TE_{03} + EH_{23}$ mode has the largest spot diameter at moderate focusing.

It is theoretically found and experimentally confirmed that transverse distribution of the total electric field intensity for the $TE_{01q} + EH_{21q}$ mode of a dielectric waveguide resonator preserves a ring shape in the region of the minimum size of focused radiation beams. This characteristic remains unchanged at both moderate and sharp focusing.

References

1. Akyildiz I.F., Han C., Hu Z. *et al*. Terahertz band communication: an old problem revisited and research directions for the next decade. *IEEE Trans. Commun*. 2020. **70**. P. 4250–428. https://doi.org/10.1109/TCOMM.2022.3171800.
2. Castro-Camus E., Koch M., Mittleman D.M. Recent advances in terahertz imaging: 1999 to 2021. *Appl. Phys. B*. 2022. **128**. P. 12. https://doi.org/10.1007/s00340-021-07732-4.
3. Saha A., Biswas A., Ghosh K., Mukhopadhyay N. *Optical to Terahertz Engineering*. Springer, 2023.
4. Cimbri D., Wang J., Al-Khalidi A., Wasige E. Resonant tunneling diodes high-speed terahertz wireless communications – a review. *IEEE Trans. Terahertz Sci. Technol*. 2022. **12**. P. 226–244. https://doi:10.1109/TTHZ.2022.3142965.
5. Alqaraghuli A.J., Siles J.V., Jornet J.M. The road to high data rates in space: terahertz versus optical wireless communication. *IEEE Aerosp. Electron. Syst. Mag*. 2023. **38**. P. 4–13. https://doi:10.1109/MAES.2023.3243584.
6. Matsumoto H., Watanabe H., Kasamatsu A., Monnai Y. Integrated terahertz radar based on leaky-wave coherence tomography. *Nat. Electron*. 2020. **3**. P. 122–129. https://doi.org/10.1038/s41928-019-0357-4.
7. Komandin G.A., Lebedev G.A., Korableva S.L. *et al*. Optical properties of $LiGdF_4$ single crystal in the terahertz and infrared ranges. *Photonics*. 2023. **10**. P. 84. https://doi.org/10.3390/photonics10010084.
8. Olivieri L., Gongora J.S.T., Peters L. *et al*. Hyperspectral terahertz microscopy via nonlinear ghost imaging. *Optica*. 2020. **7**. P. 186–196. https://doi.org/10.1364/OPTICA.381035.
9. Son J.-H., Oh S.J., Cheon H. Potential clinical applications of terahertz radiation. *J. Appl. Phys*. 2019. **125**. P. 190901. https://doi.org/10.1063/1.5080205.
10. Wu L., Wang Y., Li H. *et al*. Optimization for continuous-wave terahertz reflection imaging for biological tissues. *J. Biophotonics*. 2021. **15**. P. e202100245. https://doi.org/10.1002/jbio.202100245.
11. D'Arco A., Di Fabrizio M., Dolci V. *et al*. Characterization of volatile organic compounds (VOCs) in their liquid-phase by terahertz time-domain spectroscopy. *Biomed. Opt. Express*. 2020. **11**. P. 1–7. https://doi.org/10.1364/BOE.11.000001.
12. Leitenstorfer A., Moskalenko A.S., Kampfrath T. *et al*. The 2023 terahertz science and technology roadmap. *J. Phys. D: Appl. Phys*. 2023. **56**. P. 223001. https://doi.org/10.1088/1361-6463/acbe4c.
13. Valusis G., Lisauskas A., Yuan H. *et al*. Roadmap of terahertz imaging. 2021. *J. Sensors*. 2021. **21**. P. 4092. https://doi.org/10.3390/s21124092.
14. Kallioniem L., Turquet L., Lipsanen H. *et al*. Tailoring the longitudinal electric fields of high-order laser beams and their direct verification in three dimensions. *Opt. Commun*. 2020. **459**. P. 124894. https://doi.org/10.1016/j.optcom.2019.124894.
15. Fu J., Yu X., Wang Y., Chen P. Generation of pure longitudinal magnetization needle with tunable longitudinal depth by focusing azimuthally polarized beams. *Appl. Phys. B*. 2018. **124**. P. 11. https://doi.org/10.1007/s00340-017-6886-5.
16. Kozawa Y., Sato S. Sharper focal spot formed by higher-order radially polarized laser beams. *J. Opt. Soc. Am*. 2007. **24**. P. 1793–1798. https://doi.org/10.1364/JOSAA.24.001793.
17. Jin X., Zgang H., Xu Y. *et al*. Representation and focusing properties of higher-order radially polarized Laguerre–Gaussian beams. *J. Mod. Opt*. 2015. **62**. P. 626–632. https://doi.org/10.1080/09500340.2014.999138.
18. Zhan Q. Cylindrical vector beams: from mathematical concepts to applications. *Adv. Opt. Photon*. 2009. **1**. P. 1–57. https://doi.org/10.1364/AOP.1.000001.
19. Degtyarev A.V., Dubinin M.M., Gurin O.V. *et al*. Control of tightly focused laser beams in the THz range. *Microw. Opt. Technol. Lett*. 2021. **3**. P. 2888–2892. https://doi.org/10.1002/mop.32946.
20. Gurin O.V., Degtyarev A.V., Dubinin M.M. *et al*. Focusing of modes with an inhomogeneous spatial polarization of the dielectric resonator of a terahertz laser. *Telecommun. Radio Eng*. 2020. **79**. P. 105–116. https://doi.org/10.1615/TelecomRadEng.v79.i2.30.
21. Winnerl S., Hubrich R., Mittendorff M. *et al*. Universal phase relation between longitudinal and transverse fields observed in focused terahertz beams. *New J. Phys*. 2012. **14**. P. 2–12. https://doi.org/10.1088/1367-2630/14/10/103049.
22. Winnerl S., Hubrich R., Mittendorff M. et al. Longitudinal terahertz wave generation from an air plasma filament induced by a femtosecond laser. *Appl. Phys. Lett*. 2013. **102**. P. 151106. https://doi.org/10.1063/1.4802482.
23. Yang M., Ruan D., Du L. *et al*. Subdiffraction focusing of total electric fields of terahertz wave. *Opt. Commun*. 2020. **458**. P. 124764. https://doi.org/10.1016/j.optcom.2019.124764.
24. Degtyarev A., Dubinin M., Gurin O. *et al*. Control over higher-order transverse modes in a waveguide-based quasi-optical resonator. *Radio Phys. Radio Astron*. 2022. **27**. P. 129–139. https://doi.org/10.15407/rpra27.02.129.
25. Henningsen J., Hammerich M., Olafsson A. Mode structure of hollow dielectric waveguide lasers. *Appl. Phys. B*. 1990. **51**. P. 272–284. https://doi.org/10.1007/BF00325048.
26. Luneburg R.K. *Mathematical Theory of Optics*. University of California Press, 1966.
27. Marcatili E.A.J., Schmeltzer R.A. Hollow metallic and dielectric waveguides for long distance optical

transmission and lasers. *Bell Syst. Tech. J.* 1964. **43**. P. 1783–1809. https://doi.org/10.1002/j.1538-7305.1964.tb04108.x.
28. Goodman J.W. *Introduction to Fourier Optics.* McGraw-Hil, 1996.
29. Dorn R., Quabis S., Leuchs G. Sharper focus for a radially polarized light beam. *Phys. Rev. Lett.* 2003. **91**. P. 233901. https://doi.org/10.1103/PhysRevLett.91.233901.
30. Kozawa Y., Sato S. Small focal spot formation by vector beams. *Prog. Opt*. 2021. **66**. P. 35–90. https://doi.org/10.1016/bs.po.2021.01.001.
31. Greivenkamp J.E. *Field Guide to Geometrical Optics*. SPIE, 2004.
32. Gurin O.V., Degtyarev A.V., Dubinin N.N. *et al*. Formation of beams with nonuniform polarisation of radiation in a cw waveguide terahertz laser. *Quantum Electron*. 2021. **51**. P. 338–342. https://doi.org/10.1070/QEL17511.
33. Degtyarev A., Maslov V., Topkov A. *Continuous-wave Terahertz Waveguide Lasers*. LAP LAMBERT Academic Publ., 2020.

Authors and CV

Andrey V. Degtyarev, PhD in Physics and Mathematics, Associate Professor, Department of Quantum Radiophysics, School of Radiophysics, Biomedical Electronics and Computer System of the V. Karazin Kharkiv National University. He is the author of more than 80 scientific works, several methodical training manuals, three monographs, and a patent for an invention. The field of his scientific interests is laser physics, laser optics, and propagation of laser radiation beams in electromagnetic energy transmission lines.
E-mail: a.v.degtyarev@karazin.ua,
https://orcid.org/0000-0003-0844-4282

Vyacheslav O. Maslov, Doctor of Physical and Mathematical Sciences, Professor, Head of the Department of Quantum Radiophysics, School of Radiophysics, Biomedical Electronics and Computer System of the V. Karazin Kharkiv National University. He is the author of more than 180 scientific works, 6 monographs, several methodical training manuals, and 16 copyright certificates for inventions and patents. The field of his scientific interests is laser physics, laser optics, and propagation of laser radiation beams in electromagnetic energy transmission lines.
E-mail: v.a.maslov@karazin.ua,
https://orcid.org/0000-0001-7743-7006

Mykola M. Dubinin, PhD in Applied Physics and Nanomaterials, Department of Quantum Radiophysics, School of Radiophysics, Biomedical Electronics and Computer System at the V. Karazin Kharkiv National University. He is the author of more than 30 scientific works. The field of his scientific interests is laser physics, laser optics, propagation, focusing and control of laser radiation beams.
https://orcid.org/0000-0002-7723-9592

Oleg V. Gurin, Researcher, Department of Quantum Radiophysics, School of Radiophysics, Biomedical Electronics and Computer System of the V. Karazin Kharkiv National University. He is the co-author of 40 scientific publications and 6 innovations. The field of his scientific interests is formation of beams with uniform intensity distribution and transverse mode selection in laser cavities. He is also engaged in the research on the effects of submillimeter radiation on biological objects.
E-mail: oleg.v.gurin@i.ua,
https://orcid.org/0000-0003-1382-5338

Konstantin I. Muntean, Researcher, Department of Quantum Radiophysics, School of Radiophysics, Biomedical Electronics and Computer System of the V. Karazin Kharkiv National University. He is the author and co-author of more than 90 scientific publications, including 14 copyright certificates and patents for inventions. The field of his scientific interests is measurement and stabilization of laser radiation parameters.
E-mail: k.i.muntean@karazin.ua,
https://orcid.org/0000-0001-6479-3511

Valery N. Ryabykh, Researcher, Department of Quantum Radiophysics, School of Radiophysics, Biomedical Electronics and Computer System of the V. Karazin Kharkiv National University. He is the co-author of 30 scientific publications and six innovations. The field of his scientific interests is formation of beams with uniform intensity distribution and transverse mode selection in laser cavities. He is also engaged in the research on the effects of submillimeter radiation on biological objects.
E-mail: v.ryabykh@karazin.ua,
https://orcid.org/0000-0002-3526-292X

Oleh O. Svystunov, PhD Student, Department of Quantum Radiophysics, School of Radiophysics, Biomedical Electronics and Computer System at the V. Karazin Kharkiv National University. He is the author of 5 scientific works. The field of his scientific interests is laser physics, laser optics, propagation and focusing of laser radiation beams.
E-mail: oleg.svistunov.98@gmail.com,
https://orcid.org/0000-0002-4967-5944

Vladislav S. Senyuta, PhD in Physics and Mathematics, Senior Research Scientist, Department of Quantum Radiophysics, School of Radiophysics, Biomedical Electronics and Computer System at the V. Karazin Kharkiv National University. Authored of more than 40 scientific works. The field of his scientific interests is laser physics, laser optics, and propagation of laser radiation beams in electromagnetic energy transmission lines.
E-mail: v.s.senyuta@karazin.ua,
https://orcid.org/0000-0001-6601-2379

Authors' contributions

Degtyarev A.V.: formal analysis, project administration, writing – review & editing.
Dubinin M.M.: methodology, investigation, data curation, writing – review & editing.
Gurin O.V.: investigation, formal analysis.
Maslov V.A.: formal analysis, conceptualization, investigation, writing – original draft, writing – review & editing.
Muntean K.I.: validation, formal analysis
Ryabykh V.N.: investigation, formal analysis.
Senyuta V.S.: validation, formal analysis.
Svystunov O.O.: investigation, formal analysis.

Властивості сфокусованих комбінованих мод терагерцового лазера

А.В Дегтярьов, М.М. Дубінін, О.В. Гурін, В.О. Маслов, К.І. Мунтян, В.М. Рябих, В.С. Сенюта
О.О. Свистунов

Анотація. Теоретично та експериментально проаналізовано фізичні особливості просторово-енергетичних характеристик ТГц лазерних пучків з лінійною поляризацією поля при гострому та помірному фокусуванні у вільному просторі. Векторна теорія Релея–Зоммерфельда була використана для моделювання поширення у вільному просторі лазерних пучків, збуджених модами квазіоптичного хвилевідного резонатора. Для експериментального дослідження використано відомі методи вимірювання просторово-енергетичних характеристик лазерних пучків ТГц діапазону. Показано, що сумарна інтенсивність поля комбінованих $TE_{0n} + EH_{2n}$ і $EH_{-1n} + EH_{3n}$ (n = 1, 2, 3) мод визначається усіма трьома компонентами і має провал на осі для обох типів фокусування. Центральні максимуми поля цих мод значно зміщуються від геометричних фокусів досліджуваних лінз зі збільшенням порядку n цих мод. Найменший діаметр фокальної плями в області максимальної інтенсивності при гострому фокусуванні. має мода $EH_{-11} + EH_{31}$ (2,94λ). Мода $TE_{01} + EH_{21}$ має найменший діаметр (13,65λ) фокусної плями при помірному фокусуванні.

Ключові слова: терагерцовий лазер, діелектричний резонатор, комбіновані моди, поляризація, фокусування.